

Ferromagnetic order in the electron-doped system $\text{La}_{1-x}\text{Ce}_x\text{CoO}_3$

D. Fuchs,¹ P. Schweiss,¹ P. Adelman,¹ T. Schwarz,^{1,2} and R. Schneider¹

¹Forschungszentrum Karlsruhe, Institut für Festkörperphysik, P. O. Box 3640, D-76021 Karlsruhe, Germany

²Universität Karlsruhe, Fakultät für Physik, D-76128 Karlsruhe, Germany

(Received 4 March 2005; revised manuscript received 23 May 2005; published 28 July 2005)

Highly *electron*-doped cobaltites of the system $\text{La}_{1-x}\text{Ce}_x\text{CoO}_3$ ($0.1 \leq x \leq 0.4$) are synthesized by the growth of epitaxial thin films using pulsed laser deposition. Ferromagnetic order is observed within the entire doping range with the maximum of the Curie temperature, T_c , at $x \approx 0.3$, resulting in a magnetic phase diagram similar to that of hole-doped lanthanum cobaltites. The measured spin values strongly suggest an intermediate-spin state of the Co ions which has been also found in the hole-doped system. However, in contrast to the hole-doped material, where T_c is well above 200 K, we observe a strong suppression of the maximum T_c to about 22 K. This is likely to be caused by a considerable decrease of the Co 3d–O 2p hybridization. The observed intriguing magnetic properties are in agreement with previously reported theoretical results.

DOI: 10.1103/PhysRevB.72.014466

PACS number(s): 75.70.-i, 75.47.Gk, 75.47.Pq

I. INTRODUCTION

The hole-doped rare-earth cobaltites $\text{R}_{1-x}\text{A}_x\text{CoO}_3$ (R=trivalent rare-earth element, A=divalent alkaline-earth element) have attracted a lot of attention due to their interesting magnetic properties. The evolution of magnetism with the hole-doping level x and with temperature is governed by the transition from the spin-glass-like state to a cluster-glass state or to the ferromagnetic (FM) metallic state,^{1,2} where double exchange, involving Co ions in different charge states, provides the magnetic coupling. In addition to the lattice, charge, and spin degrees of freedom found in the manganites and many other transition metal oxides, the cobaltites also display a degree of freedom in the spin state of the Co ion. Since Hund's coupling constant is comparable to the crystal field splitting, various spin states are possible, such as low-spin (LS) $t^6_2g e^0_g$, $S=0$, intermediate-spin (IS) $t^5_2g e^1_g$, $S=1$, and high-spin state (HS) $t^4_2g e^2_g$, $S=2$, which are favored by large crystal-field splitting, covalency, and exchange energy, respectively.^{3,4} The question we want to address in this paper is how electron doping affects the magnetic properties of the cobaltite perovskites. To this end, we substituted the trivalent rare-earth La^{3+} by tetravalent Ce^{4+} ions.

Perovskite samples of the formula $\text{La}_{1-x}\text{Ce}_x\text{CoO}_3$ are known as catalysts for exhaust gas depollution.⁵ The preparation and properties of compounds with small $x \leq 0.03$ have already been discussed by Tabata and Kido.⁶ A transition to a ferromagnetic state was not observed by the authors. To our knowledge, the preparation of *single phase* bulk material $\text{La}_{1-x}\text{Ce}_x\text{CoO}_3$ with a higher doping level, i.e., $x > 0.03$, has not been achieved up to now. Mitra *et al.*⁷ already succeeded in the preparation of cerium doped manganites by the growth of thin films and demonstrated the electron doping of $\text{La}_{0.7}\text{Ce}_{0.3}\text{MnO}_3$ by x-ray absorption measurements.⁸ $\text{La}_{0.7}\text{Ce}_{0.3}\text{MnO}_3$ displays properties remarkably similar to the hole-doped system $\text{La}_{0.7}\text{Ca}_{0.3}\text{MnO}_3$, i.e., a ferromagnetic metallic ground state with a T_c and a metal-insulator transition at about 250 K.⁹ This indicates a similar behavior of the mixed valent states of Mn^{3+} – Mn^{4+} (hole doping) and Mn^{3+} – Mn^{2+} (electron doping). An intuitive explanation suggests that, due to the splitting of the spin- e_g states of the

Mn^{3+} ion ($t^3_g e^1_g$), hole and electron doping x create the same amount of free charge carriers in the e_g band which mediate the double exchange interaction.

In the cobaltites, the situation is more complicated due to the different possible Co spin states. Zhang *et al.*¹⁰ have carried out theoretical investigations on the magnetic structure of $\text{La}_{1-x}\text{Ce}_x\text{CoO}_3$ and postulate a LS state for $x < 0.08$ and a LS-IS ferromagnetically ordered state for $0.08 \leq x < 0.83$.

In this work, we report on the synthesis of highly electron-doped cobaltites by pulsed laser deposition of epitaxial thin films and their intriguing magnetic properties illuminating the spin state in comparison to the corresponding hole-doped cobaltites.

II. EXPERIMENT

For the pulsed laser deposition of $\text{La}_{1-x}\text{Ce}_x\text{CoO}_3$ ($x=0.1, 0.2, 0.3, \text{ and } 0.4$) we have used sintered targets which were prepared by the sol-gel method¹¹ in order to improve the Ce diffusion and homogeneity of the starting material. However, we did not succeed in the preparation of single phase target material, not even for $x=0.1$. For each target we observed an impurity phase of CeO_2 , increasing with the Ce concentration x . The films were deposited with a thickness of about 80 nm on $\langle 001 \rangle$ oriented LaAlO_3 single crystal substrates. We also grew films on different substrate materials, i.e., SrTiO_3 and $(\text{LaAlO}_3)_{0.3}(\text{Sr}_2\text{AlTaO}_6)_{0.7}$.

The growth conditions, i.e., substrate temperature, T_s , oxygen partial pressure, $p(\text{O}_2)$, and laser energy, E , were optimized with respect to crystallinity and magnetic properties of the resulting films. Despite the impurity phase of CeO_2 in the targets we succeeded in the growth of highly epitaxial single-phase thin films up to $x=0.4$ at $T_s = 550^\circ\text{C}$, $E=450$ mJ, and at an oxygen partial pressure of $p(\text{O}_2)=0.3$ mbar. The structural characterization was carried out by x-ray diffraction (XRD). Figure 1 demonstrates the epitaxial quality of the $\langle 001 \rangle$ oriented films. Only 00l reflections can be observed. The rocking curve at the 002 reflection, see inset of Fig. 1, reveals a mosaic spread smaller than 0.2° . The c -axis lattice parameter, $c \approx 3.84$ Å, was

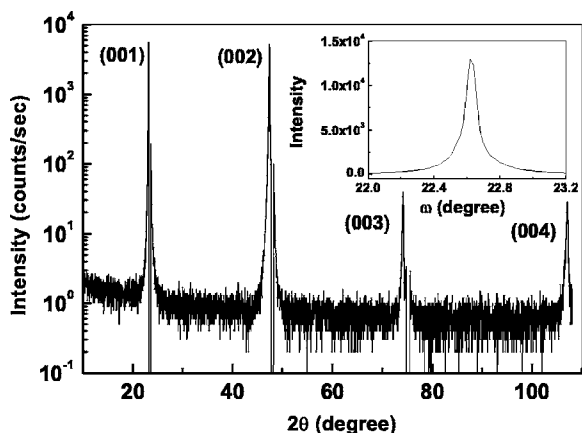


FIG. 1. $\theta/2\theta$ scan of $\text{La}_{0.7}\text{Ce}_{0.3}\text{CoO}_3$ using $\text{Cu}_{K\alpha}$. The substrate reflections of LaAlO_3 have been removed for clarity. Only $00l$ reflections of $\text{La}_{0.7}\text{Ce}_{0.3}\text{CoO}_3$ can be observed. The inset shows an ω scan at the 002 reflection. The full width at half maximum amounts to 0.15° .

found to be nearly constant within the doping range and larger than the bulk value, $c_b = 3.80 \text{ \AA}$, which we determined from the target material. The difference is likely to be caused by an in-plane compressive strain due to the epitaxial growth on LaAlO_3 substrates with an in-plane lattice parameter of 3.78 \AA . For thick films with $d > 300 \text{ nm}$, the XRD data hint at an increased orthorhombic distortion, i.e., an asymmetric shape of the $00l$ reflections and a small peak splitting with increasing doping level x which, for thinner films, is likely to be masked by linewidth broadening due to the relaxation of epitaxial strain and finite size effects.

We also carried out transmission electron microscopy and energy dispersive x-ray (EDX) analysis on various sample positions confirming the microstructural and chemical homogeneity of the films. In Fig. 2 we display an EDX line scan analysis of a $\text{La}_{0.7}\text{Ce}_{0.3}\text{CoO}_3$ film. The x-ray fluorescence intensity coming from the La_L , Ce_L , and Co_K shell is plotted as a function of the distance in the film plane. The intensity ratio $[I(\text{La}_L) + I(\text{Ce}_L)]/I(\text{Co}_K)$ is nearly constant over the entire distance of about 200 nm and amounts to about 1, indi-

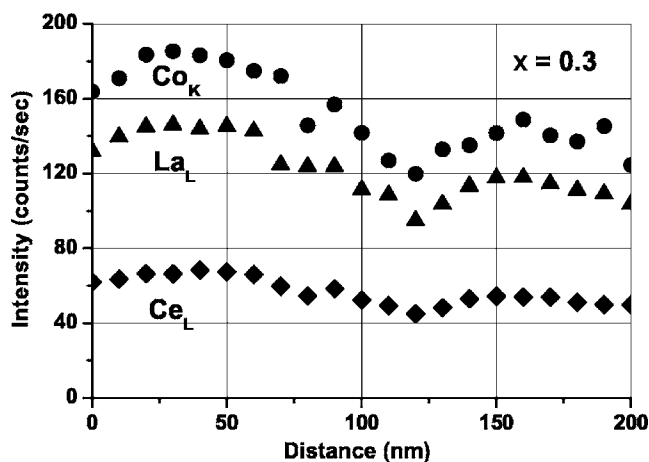


FIG. 2. Energy dispersive x-ray analysis of a $\text{La}_{0.7}\text{Ce}_{0.3}\text{CoO}_3$ film. The x-ray fluorescence intensity coming from the La_L , Ce_L , and Co_K shell is plotted as a function of distance in the film plane.

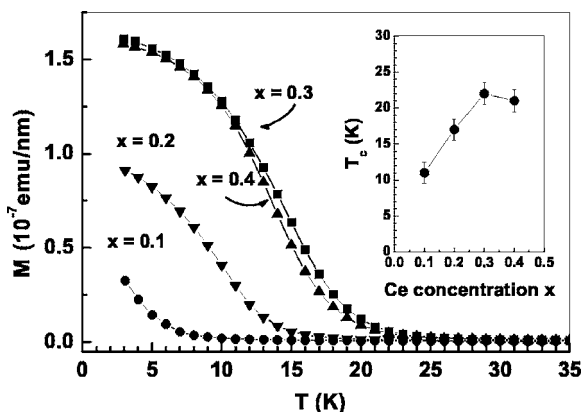


FIG. 3. Field-cooled magnetization of $\text{La}_{1-x}\text{Ce}_x\text{CoO}_3$ for $x = 0.1$ (circles), 0.2 (down triangles), 0.3 (squares), and 0.4 (up triangles). The measurements were carried out with an external field strength of $H = 200 \text{ Oe}$ applied parallel to the film surface. The inset displays the Curie temperature, T_c , determined from the onset of the field-cooled magnetization as a function of the Ce-doping level x .

cating a homogeneous and stoichiometric composition. The variation of the absolute intensity with the distance is caused by an inhomogeneous sample thickness due to the sample thinning procedure. We also carried out Rutherford back-scattering experiments to analyze the sample composition in more detail, yielding the same results.

In order to ensure a good oxygenation of the samples we carried out an oxygen annealing after film deposition in a pure oxygen atmosphere of 0.9 bar at 500°C for about 30 min.

The magnetic properties of the films were studied using a Quantum Design MPMS superconducting quantum interference device system. The zero-field-cooled and field-cooled (FC) magnetization was measured with an external field strength of $H = 200 \text{ Oe}$ applied parallel to the film surface in the temperature range of $3 \text{ K} \leq T \leq 300 \text{ K}$. Resistivity measurements were carried out in a four point contact geometry from room temperature down to 4.2 K .

III. RESULTS AND DISCUSSION

In Fig. 3, we display the FC magnetization versus temperature normalized to the film thickness for $x = 0.1, 0.2, 0.3,$ and 0.4 . A transition to a ferromagnetic state is observed for all the samples. The Curie temperature, T_c , was determined from the onset of the FC magnetization and is shown as a function of the Ce-doping level in the inset of Fig. 3. With increasing electron-doping level x , T_c increases almost linearly up to $x = 0.3$, where the maximum value of $T_c \approx 22 \text{ K}$ is reached. In comparison to the hole-doped cobaltites, where the maximum T_c is 240 K for Sr doping,¹² the Curie temperature of the electron-doped samples is strongly suppressed. In order to exclude extrinsic effects as a source for the suppressed T_c , such as a poor oxygenation, bad crystallinity, epitaxial strain or finite size effects of the films, we studied in detail the influence of the deposition parameters, i.e., $p(\text{O}_2), T_s, E$, substrate material and film thickness, respectively, on T_c . An enhancement of the Curie temperature

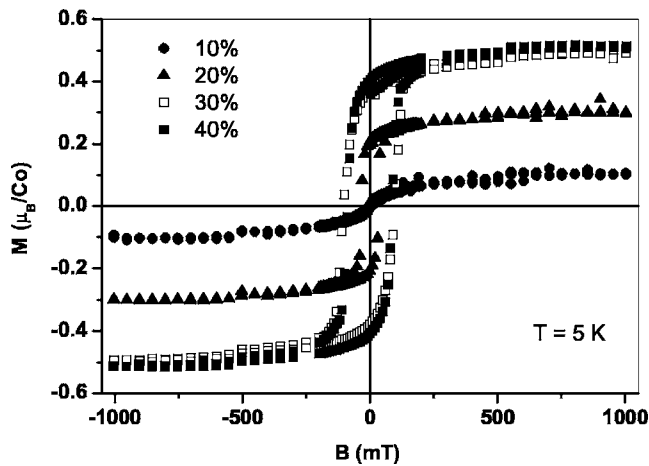


FIG. 4. The magnetization of $\text{La}_{1-x}\text{Ce}_x\text{CoO}_3$ as a function of the magnetic field, applied parallel to the film surface at $T=5$ K for different Ce-doping x .

above the optimum of $T_c \approx 22$ K was not feasible.

Nevertheless, T_c seems to saturate at the same doping concentration $x \approx 0.3$ as observed for $\text{La}_{1-x}\text{Sr}_x\text{CoO}_3$, leading to a magnetic phase diagram which is qualitatively similar to that of the hole-doped cobaltites.

In Fig. 4, we show the magnetization as a function of the magnetic field at $T=5$ K for different Ce doping. The magnetization displays well shaped hysteresis curves, indicative for a long range ferromagnetic ordering with saturation above 300 mT. With increasing Ce doping x the coercive field, H_c , increases from 5 mT for $x=0.1$ to about 100 mT for $x \geq 0.3$. The magnetic ordered moment in the ferromagnetic state was determined from the magnetic saturation at $T=5$ K and $B=5$ T and amounts to $\mu_{\text{sat}}(\text{FM}) = 0.5 \mu_B/\text{Co}$ (μ_B : Bohr magneton) for $\text{La}_{0.7}\text{Ce}_{0.3}\text{CoO}_3$. Since the magnetic moment of itinerant ferromagnets can be significantly reduced in the ferromagnetic state, we also determined the paramagnetic effective moment, μ_{eff} , in the paramagnetic state from susceptibility measurements well above T_c , i.e., $T > 50$ K.¹³ For $\text{La}_{0.7}\text{Ce}_{0.3}\text{CoO}_3$ we obtained $\mu_{\text{eff}} = 3.3 \mu_B/\text{Co}$, which is much higher than the magnetic ordered moment in the ferromagnetic state. For the hole-doped $\text{La}_{0.7}\text{Sr}_{0.3}\text{CoO}_3$, Paraskevopoulos *et al.* also measured a magnetic moment of $\mu_{\text{eff}} = 3.37 \mu_B/\text{Co}$,¹⁴ indicating that the spin configurations of these electron and hole-doped cobaltites are rather similar.

From the magnetic moment in the paramagnetic state we calculated the spin value, S , assuming $\mu_{\text{eff}} = g[S(S+1)]^{1/2} \mu_B$, with a Landé factor $g=2$. In Fig. 5, we show S as a function of the Ce-doping level x . We also display the S values which are expected for a LS state: $t^6_{2g}e^x_g$, IS state: $t^5_{2g}e^{1+x}_g$, and HS state: $t^{4+x}_{2g}e^2_g$, where $S=x/2$, $(2+x)/2$, and $(4-x)/2$, respectively,¹⁰ assuming a simple ionic picture. The measured S value increases with increasing doping level x , very similar to that of an IS state. From Fig. 5, there might be some indication for the disappearance of a residual LS state above $x \approx 0.2-0.3$. The result is in agreement with a previously published theoretical work of Zhang *et al.*,¹⁰ suggesting a LS-IS configuration for $0.08 < x < 0.83$.

Resistivity measurements indicate that the Ce-doped films are rather in a ferromagnetic insulating than in a metallic

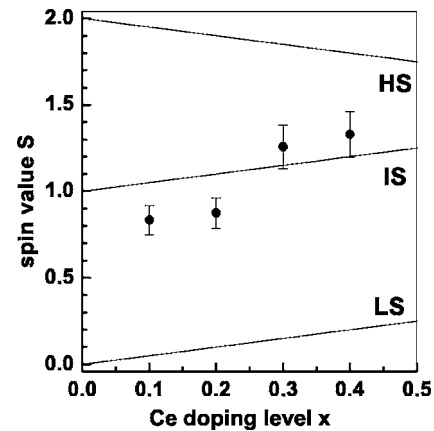


FIG. 5. The spin-value, S , calculated from μ_{eff} in the paramagnetic state, as a function of the Ce concentration x . The expected spin values for a LS state: $t^6_{2g}e^x_g$, IS state: $t^5_{2g}e^{1+x}_g$, and HS state: $t^{4+x}_{2g}e^2_g$, where $S=x/2$, $(2+x)/2$, and $(4-x)/2$, respectively, are displayed by solid lines.

state. The room temperature resistivity increases with increasing doping level from $\rho \approx 78 \Omega \text{ cm}$ for $x=0.1$ to $1.8 \times 10^3 \Omega \text{ cm}$ for $x=0.3$ and $\rho > 4 \times 10^4 \Omega \text{ cm}$ for $x=0.4$. With decreasing temperature the resistivity of the samples increased very rapidly and was so high that the current source broke down, i.e., the resistance was above the measuring range where it keeps down to the lowest measured temperature of $T=3$ K. Indications for a metal-insulator transition could not be detected.

In order to explain the high resistivity and the low T_c of Ce-doped cobaltites we suggest the following scenario: The increase of the resistivity with increasing Ce doping can probably be explained by an increase of localization of charge carriers which might be correlated with an enhanced orthorhombic distortion. It is well known that an orthorhombic distortion of the oxygen octahedra leads to charge carrier localization.¹⁵ Reasons for the orthorhombic distortion may be the decrease of the tolerance factor, $t=(A-O)/\sqrt{2(B-O)}$, where A, B, and O are the ionic radii within the ABO_3 perovskite structure, and the increase of the size mismatch of the A-site cations, i.e., La^{3+} and Ce^{4+} , with increasing x . If the La^{3+} ions ($A=1.216 \text{ \AA}$) are partially replaced by smaller Ce^{4+} ions ($A \approx 1.019 \text{ \AA}$), t decreases due to the increase of the bond-length mismatch between A-O and B-O. A bond-length mismatch can usually be compensated by a rotation about ϕ of the BO_6 octahedra around the $[110]$ axis which results in an orthorhombic distortion.¹⁶ Thus, the tilt angle, ϕ , of the oxygen octahedra also increases leading to a decrease of the hybridization among the Co $3d$ and O $2p$ bands and the bandwidth, W , which depends on the Co-O-Co bond angle ($180^\circ - \phi$) through $W \propto \cos \phi$. A decreased hybridization and bandwidth also causes a decrease of the double exchange interaction which may be the reason for the low Curie temperature in the Ce-doped cobaltites.

The size mismatch of the A-site cations can cause a disorder which induces lattice strain and a random displacement of oxygen ions, resulting in a distortion of the CoO_6 octahedra and hence the localization of electrons.

Since tolerance factor and A-site cation mismatch are comparable to the Ce-doped manganites, i.e.,

$\text{La}_{0.7}\text{Ce}_{0.3}\text{MnO}_3$, which show a T_c value very similar to that of the hole doped counterpart $\text{La}_{0.7}\text{Ca}_{0.3}\text{MnO}_3$, it is still unclear why the hybridization and T_c are so strongly suppressed in the Ce-doped cobaltites. Therefore, further experiments are planned including the characterization of the electronic band structure which will be helpful to clarify this question.

IV. SUMMARY

In summary, we have demonstrated that it is possible to obtain highly electron-doped cobaltites by the growth of ep-

itaxial thin films. The electron-doped $\text{La}_{1-x}\text{Ce}_x\text{CoO}_3$ films show ferromagnetic order within the entire doping range $0.1 \leq x \leq 0.4$ with a maximum T_c of about 22 K at $x=0.3$. The paramagnetic moment increases with increasing Ce-doping level x and indicates a stable IS configuration over the investigated doping range.

With increasing Ce doping the resistivity increases which might indicate a decrease of hybridization among Co $3d$ -O $2p$ orbitals. We suggest that the decreased hybridization is primarily caused by the orthorhombic distortion and mainly responsible for the strongly suppressed T_c in comparison to the counterdoped hole-doped cobaltites.

-
- ¹R. Caciuffo, D. Rinaldi, G. Barucca, J. Mira, J. Rivas, M. A. Señarís-Rodríguez, P. G. Radaelli, D. Fiorani, and J. B. Goodenough, *Phys. Rev. B* **59**, 1068 (1999).
- ²M. Itoh, I. Natori, S. Kubota, and K. Motoya, *J. Phys. Soc. Jpn.* **63**, 1486 (1994).
- ³M. A. Korotin, S. Y. Ezhov, I. V. Solovyev, V. I. Anisimov, D. I. Khomskii, and G. A. Sawatzky, *Phys. Rev. B* **54**, 5309 (1996).
- ⁴R. H. Potze, G. A. Sawatzky, and M. Abbate, *Phys. Rev. B* **51**, 11501 (1995).
- ⁵T. Nitadori and M. Misono, *J. Catal.* **93**, 459 (1985).
- ⁶K. Tabata and H. Kido, *Phys. Status Solidi A* **111**, K 105 (1989).
- ⁷C. Mitra, P. Raychaudhuri, J. John, S. K. Dhar, A. K. Nigam, and R. Pinto, *J. Appl. Phys.* **89**, 524 (2001).
- ⁸C. Mitra, Z. Hu, P. Raychaudhuri, S. Wirth, S. I. Csiszar, H. H. Hsieh, H. J. Lin, C. T. Chen, and L. H. Tjeng, *Phys. Rev. B* **67**, 092404 (2003).
- ⁹P. Mandal and S. Das, *Phys. Rev. B* **56**, 15073 (1997).
- ¹⁰Q. Zhang, X. Huang, W. Zhang, and A. Hu, *J. Appl. Phys.* **95**, 6822 (2004).
- ¹¹L. Ben-Dor, H. Diab, and I. Felner, *J. Solid State Chem.* **88**, 183 (1990).
- ¹²M. A. Señarís-Rodríguez and J. B. Goodenough, *J. Solid State Chem.* **118**, 323 (1995).
- ¹³For a small magnetic field strength, i.e., $H=200$ Oe, and $T \gg T_c$, the susceptibility, χ , is given by $M/H \approx N \cdot \mu_{\text{eff}}^2 / 3k_B T$, where the effective magnetic moment, μ_{eff} , can be determined from the slope of the magnetization M vs. $1/T$. N is the number of spins/ m^3 and k_B the Boltzmann constant.
- ¹⁴M. Paraskevopoulos, J. Hemberger, A. Krimmel, and A. Loidl, *Phys. Rev. B* **63**, 224416 (2001).
- ¹⁵L. M. Rodríguez Martínez and J. P. Attfield, *Phys. Rev. B* **58**, 2426 (1998).
- ¹⁶J. S. Zhou and J. B. Goodenough, *Phys. Rev. Lett.* **94**, 065501 (2005).